

Interface superconductivity in $\text{LaAlO}_3\text{-SrTiO}_3$ heterostructures

S. N. Klimin,^{*} J. Tempere,[†] and J. T. Devreese
*Theorie van Kwantumsystemen en Complexe Systemen (TQC),
 Universiteit Antwerpen, Universiteitsplein 1, B-2610 Antwerpen, Belgium*

D. van der Marel
*Département de Physique de la Matière Condensée,
 Université de Genève, CH-1211 Genève 4, Switzerland
 (Dated: April 18, 2022)*

The interface superconductivity in $\text{LaAlO}_3\text{-SrTiO}_3$ heterostructures reveals a non-monotonic behavior of the critical temperature as a function of the two-dimensional density of charge carriers. We develop a theoretical description of interface superconductivity in strongly polar heterostructures, based on the dielectric function formalism. The density dependence of the critical temperature is calculated accounting for all phonon branches including different types of optical (interface and half-space) and acoustic phonons. The LO- and acoustic-phonon-mediated electron-electron interaction is shown to be the dominating mechanism governing the superconducting phase transition in the heterostructure.

I. INTRODUCTION

Recent progress in the development of multilayer structures based on complex oxides [1], provides the means to generate a two-dimensional electron gas (2DEG) at the oxide interfaces. The discovery of superconductivity at the $\text{LaAlO}_3\text{-SrTiO}_3$ interface [2–6] has stimulated increasing interest in the experimental and theoretical study of these structures.

Because strontium titanate is a highly polar crystal, the electron-phonon mechanism of superconductivity seems to be the most promising for the explanation of the experimental data on superconductivity in the $\text{LaAlO}_3\text{-SrTiO}_3$ heterostructures. The Migdal – Eliashberg theory of superconductivity [7, 8], as well the BCS theory, is valid when the phonon frequencies are much smaller than the electron Fermi energy. This is not the case for polar crystals with sufficiently high optical-phonon frequencies, like strontium titanate. To tackle such systems, non-adiabatic extensions of the theory of superconductivity have been developed. Pietronero *et al.* [9–11] generalized the Eliashberg equations to include non-adiabatic corrections beyond Migdal’s theorem. The method developed by Kirzhnits *et al.* [12] (see also Refs. [13–15]) is focused on the superconductivity caused by the Fröhlich electron-phonon interaction with polar optical phonons. It uses the total dielectric function of a polar crystal. The Pietronero and Kirzhnits approaches are complementary: the former is non-perturbative with respect to the coupling strength and perturbative with respect to the Debye energy, while the latter is weak-coupling but

non-perturbative with respect to the optical-phonon energies.

Strontium titanate is a unique example of a polar medium in which superconductivity has been detected at very low carrier densities, so that the optical-phonon energies can be larger than the Fermi energy. Moreover, as found in Refs. [16, 17], the electron – LO-phonon coupling constant in SrTiO_3 is not very large. Therefore for the investigation of superconductivity in a $\text{LaAlO}_3\text{-SrTiO}_3$ heterostructure, the Kirzhnits method seems to be appropriate. Here, we apply the Kirzhnits method for a multilayer structure with several polar layers.

II. SUPERCONDUCTIVITY IN A MULTILAYER POLAR STRUCTURE

We consider the quasi 2D electron-phonon system described by the Hamiltonian:

$$\begin{aligned}
 H = & \sum_{\mathbf{k}_{\parallel}} \sum_{\sigma, j} \epsilon_{j, n, \mathbf{k}_{\parallel}} c_{\sigma, j, n, \mathbf{k}_{\parallel}}^+ c_{\sigma, j, n, \mathbf{k}_{\parallel}} \\
 & + \frac{1}{2L^2} \sum_{\mathbf{k}_{\parallel}, \mathbf{k}'_{\parallel}} \sum_{\mathbf{q}} \sum_{\sigma, j, n, \sigma', j', n'} U_{\mathbf{q}}^{(n', n)} \\
 & \times c_{\sigma, j, n, \mathbf{k}_{\parallel} + \mathbf{q}}^+ c_{\sigma', j', n', \mathbf{k}'_{\parallel}}^+ c_{\sigma', j', n', \mathbf{k}'_{\parallel} + \mathbf{q}} c_{\sigma, j, n, \mathbf{k}_{\parallel}} \\
 & + \sum_{\mathbf{q}} \sum_{\lambda} \hbar \Omega_{\mathbf{q}, \lambda} a_{\mathbf{q}, \lambda}^+ a_{\mathbf{q}, \lambda} \\
 & + \frac{1}{L} \sum_{\mathbf{q}, \lambda} \left(\gamma_{\mathbf{q}, \lambda} a_{\mathbf{q}, \lambda} + \gamma_{\mathbf{q}, \lambda}^+ a_{\mathbf{q}, \lambda}^+ \right). \quad (1)
 \end{aligned}$$

Here $a_{\mathbf{q}, \lambda}, a_{\mathbf{q}, \lambda}^+$ are the phonon second quantization operators, \mathbf{q} is the 2D in-plane phonon wave vector, the index λ labels phonon branches in the LAO-STO structure, $\Omega_{\lambda}(\mathbf{q})$ is the phonon frequency. Furthermore, $c_{\sigma, j, n, \mathbf{k}_{\parallel}}^+$ and $c_{\sigma, j, n, \mathbf{k}_{\parallel}}$ are, respectively, the creation and annihilation operators for electrons with spin σ , in-plane wave

^{*}On leave of absence from: Department of Theoretical Physics, State University of Moldova, str. A. Mateevici 60, MD-2009 Kishinev, Republic of Moldova.

[†]Also at Lyman Laboratory of Physics, Harvard University, Cambridge, MA 02138, USA.

vector \mathbf{k}_{\parallel} , band index j and size-quantization quantum number n . The energy corresponding to the single-particle state $|j, n, \mathbf{k}_{\parallel}\rangle$ is $\epsilon_{j,n,\mathbf{k}_{\parallel}}$. L is the lateral size of the system, and $U_{\mathbf{q}}^{(n',n)}$ is the matrix element of the electron-electron interaction potential,

$$U_{\mathbf{q}}^{(n',n)} = \int dz \int dz' \tilde{U}_C(q, z, z') \times \varphi_n(z) \varphi_{n'}(z) \varphi_n(z') \varphi_{n'}(z'). \quad (2)$$

The electron-phonon interaction amplitudes can be written as:

$$\gamma_{\mathbf{q},\lambda} = \sum_{j,n,j',n'} \Gamma_{\mathbf{q},\lambda}^{(n',n)} \sum_{\sigma} c_{\sigma,j',n',\mathbf{k}_{\parallel}+\mathbf{q}}^+ c_{\sigma,j,n,\mathbf{k}_{\parallel}}. \quad (3)$$

where $\Gamma_{\mathbf{q},\lambda}^{(n',n)} = \langle \varphi_{n'} | \Gamma_{\lambda}(\mathbf{q}, z) | \varphi_n \rangle$ is the matrix element of the amplitude $\Gamma_{\lambda}(\mathbf{q}, z)$ that we will specify below. The index λ labels the phonon branches of the multilayer structure. In the calculations, we assume that in the LaAlO₃-SrTiO₃ heterostructure under consideration, the electron gas is confined to a very thin layer ~ 2 nm. Consequently, only the lowest energy subband ($n = 0$) is filled, and transitions to higher subbands can be neglected.

The electron-electron interaction potential $\tilde{U}_C(q, z, z')$, the equations for the eigenfrequencies of the interface modes, and the amplitudes of the electron-phonon interaction in a multilayer structure are derived within the dielectric continuum approach accounting for the electrostatic boundary conditions in a similar way as in Refs. [19, 20]. We use Feynman units: $\hbar = 1$, $m_b = 1$, $\omega_0 = 1$, where ω_0 is an effective LO-phonon frequency (taken equal to the highest of the LO-phonon frequencies of SrTiO₃). The potential $\tilde{U}_C(q, z, z')$ is

$$\tilde{U}_C(q, z, z') = \frac{1}{L} \frac{2\sqrt{2}\pi\alpha_0}{\epsilon_{1,\infty}q} \left[e^{-q|z-z'|} + C_I e^{q(z+z')} \right], \quad (4)$$

expressed using the dimensionless Coulomb coupling constant

$$\alpha_0 = \frac{e^2}{2\hbar\omega_0} \left(\frac{2m_b\omega_0}{\hbar} \right)^{1/2}. \quad (5)$$

The coefficient C_I depends on the dielectric constants of the media constituting the heterostructure. For the system without an electrode at the LaAlO₃-vacuum interface, C_I is

$$C_I = \frac{\epsilon_{1,\infty}\epsilon_{3,\infty} - \epsilon_{2,\infty}^2 + \epsilon_{2,\infty}(\epsilon_{1,\infty} - \epsilon_{3,\infty}) \coth(ql)}{\epsilon_{1,\infty}\epsilon_{3,\infty} + \epsilon_{2,\infty}^2 + \epsilon_{2,\infty}(\epsilon_{1,\infty} + \epsilon_{3,\infty}) \coth(ql)}, \quad (6)$$

where l is the width of the LaAlO₃ layer. The index $s = 1, 2, 3$ in the dielectric constant $\epsilon_{s,\infty}$ labels the layers: $s = 1$ for the SrTiO₃ substrate, $s = 2$ for the LaAlO₃

layer, and $s = 3$ for the vacuum. For the system with an electrode, C_I is obtained from (6) in the limit $\epsilon_{3,\infty} \rightarrow \infty$.

We take into account the following phonon branches: (1) the interface optical phonons, (2) the half-space optical phonons, and (3) the acoustic phonons. For the interface optical phonons, the eigenfrequencies are found from the equation

$$\nu_1(\Omega_{\lambda}) \nu_2(\Omega_{\lambda}) - \mu_2^2(\Omega_{\lambda}) = 0 \quad (7)$$

with the functions

$$\nu_1(\Omega_{\lambda}) = \epsilon_1(\Omega_{\lambda}) + \epsilon_2(\Omega_{\lambda}) \coth(ql), \quad (8)$$

$$\nu_2(\Omega_{\lambda}) = \epsilon_2(\Omega_{\lambda}) \coth(ql) + \epsilon_3(\Omega_{\lambda}), \quad (9)$$

$$\mu_2(\Omega_{\lambda}) = \frac{\epsilon_2(\Omega_{\lambda})}{\sinh(ql)}. \quad (10)$$

The amplitudes of the electron-phonon interaction with these interface phonon modes are

$$\begin{aligned} \Gamma_{\lambda}(\mathbf{q}, z) = & \left(2\sqrt{2}\pi\alpha_0 \right)^{1/2} \left(\frac{1}{q} \frac{\Omega_{\lambda}}{D(\Omega_{\lambda})} \right)^{1/2} \\ & \times \left[e^{qz} \Theta(-z) + \frac{\nu_1(\Omega_{\lambda})}{\mu_2(\Omega_{\lambda})} e^{q(l-z)} \Theta(z-l) \right. \\ & + \Theta(z) \Theta(l-z) \\ & \left. \times \left(\frac{\sinh[q(l-z)]}{\sinh(ql)} + \frac{\nu_1(\Omega_{\lambda})}{\mu_2(\Omega_{\lambda})} \frac{\sinh(qz)}{\sinh(ql)} \right) \right] \quad (11) \end{aligned}$$

where $\Theta(z)$ is the Heaviside step function, and the factor $D(\Omega_{\lambda})$ is

$$\begin{aligned} D(\Omega_{\lambda}) = & (\epsilon_{1,0} - \epsilon_{1,\infty}) \left(\frac{\Omega_{\lambda}\omega_{1,TO}}{\Omega_{\lambda}^2 - \omega_{1,TO}^2} \right)^2 \\ & + (\epsilon_{2,0} - \epsilon_{2,\infty}) \left(\frac{\Omega_{\lambda}\omega_{2,TO}}{\Omega_{\lambda}^2 - \omega_{2,TO}^2} \right)^2 \\ & \times \frac{\left(\left(\frac{\nu_1(\Omega_{\lambda})}{\mu_2(\Omega_{\lambda})} \right)^2 + 1 \right) \cosh(ql) - 2 \frac{\nu_1(\Omega_{\lambda})}{\mu_2(\Omega_{\lambda})}}{\sinh(ql)} \\ & + (\epsilon_{3,0} - \epsilon_{3,\infty}) \left(\frac{\Omega_{\lambda}\omega_{3,TO}}{\Omega_{\lambda}^2 - \omega_{3,TO}^2} \right)^2 \left(\frac{\nu_1(\Omega_{\lambda})}{\mu_2(\Omega_{\lambda})} \right)^2. \quad (12) \end{aligned}$$

For the structure with an electrode, we set $\epsilon_3(\omega) \rightarrow \infty$ in the above formulae.

Because the 2DEG layer is positioned at the SrTiO₃ side of the interface, the half-space phonons of strontium titanate can contribute to superconductivity. The frequencies of the half-space phonons are the same as for the bulk LO phonons. The amplitudes of the electron-phonon interaction for the half-space phonons differ from those for the bulk LO phonons only by the boundary condition of zero amplitude at the interface. Although the half-space phonons turn out to give a relatively very

small contribution to the resulting phonon-mediated interaction potential, we take them into account for completeness. For the acoustic-phonon contribution, we use the frequencies and interaction amplitudes for the deformation potential from Ref. [21]:

$$\omega_{\mathbf{q}} = vq, \quad (13)$$

$$V_{\mathbf{q}}^{(ac)} = (4\pi\alpha_{ac})^{1/2} \frac{\hbar^2}{m_b} q^{1/2} \quad (14)$$

with the dimensionless coupling constant

$$\alpha_{ac} = \frac{D^2 m_b^2}{8\pi\rho\hbar^3 v}, \quad (15)$$

where ρ is the mass density of strontium titanate, D is the deformation potential, and v is the sound velocity.

The calculation of the superconducting transition temperature is performed following the scheme of Refs. [12–15] using the gap equation

$$\Delta(\omega) = - \int_{-\epsilon_F}^{\infty} \frac{d\omega'}{2\omega'} \tanh\left(\frac{\beta\omega'}{2}\right) \Delta(\omega') K(\omega, \omega') \quad (16)$$

with the kernel function

$$K(\omega, \omega') = \frac{m_b}{\pi^3} \int_0^\pi d\varphi \int_0^\infty d\Omega \frac{|\omega| + |\omega'|}{\Omega^2 + (|\omega| + |\omega'|)^2} \times V^{tot}(q, i\Omega), \quad (17)$$

where $q = \sqrt{p^2 + k^2 - 2pk \cos \varphi}$, $p = \sqrt{2m_b(\omega + \epsilon_F)}$, $k = \sqrt{2m_b(\omega' + \epsilon_F)}$, m_b is the effective mass for the motion along the surface, and $V^{tot}(q, i\Omega)$ is the total effective electron-electron interaction potential. The energy ω is counted from the Fermi energy ϵ_F . The kernel function (17) is essentially energy-nonlocal, as distinct from the BCS and Migdal – Eliashberg approaches, since it is provided by a retarded effective electron-electron interaction $V^{tot}(q, i\Omega)$, through the plasmon-phonon excitations. Consequently, the frequency dependence of the gap $\Delta(\omega)$ can differ from that within the BCS or Migdal-Eliashberg pictures.

The gap equation (16) with the effective interaction potential described above allows for the determination of the gap function $\Delta(\omega)$ and the critical temperature in a $\text{LaAlO}_3\text{-SrTiO}_3$ heterostructure. In the low-temperature range, when the thermal energy $k_B T$ is much lower than the Fermi energy of the charge carriers ϵ_F , the approximation method proposed by Zubarev [18] allows to find the normalized gap function $\phi(\omega) \equiv \Delta(\omega)/\Delta(0)$ as a numeric solution of the Fredholm equation,

$$\begin{aligned} & \phi(\omega) + \int_{-\epsilon_F}^{\infty} d\omega' \phi(\omega') \\ & \times \frac{1}{2|\omega'|} \left[K(\omega, \omega') - \frac{K(\omega, 0) K(0, \omega')}{K(0, 0)} \right] \\ & = \frac{K(\omega, 0)}{K(0, 0)}. \end{aligned} \quad (18)$$

The critical temperature is given by the expression,

$$T_c = \frac{2}{\pi} e^\gamma \epsilon_F \exp\left(-\frac{1}{\lambda}\right) \approx 1.14 \epsilon_F \exp\left(-\frac{1}{\lambda}\right), \quad (19)$$

where $\gamma = 0.577216\dots$ is the Euler constant, and the parameter λ is determined explicitly through the normalized gap parameter

$$\begin{aligned} \frac{1}{\lambda} = & - \left\{ \frac{1}{K(0, 0)} + \int_{-\epsilon_F}^{\infty} \frac{d\omega}{2|\omega|} \right. \\ & \left. \times \left[\frac{K(0, \omega)}{K(0, 0)} \phi(\omega) - \Theta(\epsilon_F - \omega) \right] \right\}. \end{aligned} \quad (20)$$

with the Heaviside step function $\Theta(\epsilon_F - \omega)$. Formulae (18) and (19) describe the relation between the kernel function $K(\omega, \omega')$, the normalized gap function $\phi(\omega)$ and the critical temperature.

In the present treatment, the effective electron-electron interaction includes contributions from both optical and acoustic phonons. Since the Kirzhnits theory assumes the weak-coupling regime, we suggest that the effective phonon-mediated interaction due to the acoustic phonons can be taken into account in an additive way with respect to the combined contribution of Coulomb interaction and optical phonons. The total effective interaction $V^{tot}(q, \Omega)$ can be thus approximated by the sum:

$$V^{tot}(q, i\Omega) = V^R(q, i\Omega) + V^{ac}(q, i\Omega), \quad (21)$$

where $V^R(q, \Omega)$ is the effective interaction described in terms of the total dielectric function, and $V^{ac}(q, i\Omega)$ is the effective interaction due to the acoustic phonons.

The effective potential $V^R(q, i\Omega)$ in a quasi 2D system is determined following Ref. [15]. Within RPA [22], the relation between the effective potential taking into account dynamic screening, $V^R(q, i\Omega)$, and the effective potential without screening, $V_0^R(q, i\Omega)$, is

$$V^R(q, i\Omega) = \frac{V_0^R(q, i\Omega)}{1 + V_0^R(q, i\Omega) P^{(1)}(q, i\Omega)} \quad (22)$$

where $P^{(1)}(q, i\Omega)$ is the polarization function of a free 2DEG. Here, we use the RPA-polarization function [13, 22, 23]. The non-screened potential $V_0^R(q, i\Omega)$ is a sum of a Coulomb contribution and a contribution from the phonon mediated interaction between the two electrons:

$$V_0^R(q, i\Omega) = U_{\mathbf{q}}^{(0,0)} - \sum_{\lambda} \frac{2\Omega_{\lambda}(q)}{\Omega_{\lambda}^2(q) + \Omega^2} \left| \Gamma_{\mathbf{q}, \lambda}^{(0,0)} \right|^2 \quad (23)$$

where the Coulomb contribution $U_{\mathbf{q}}^{(0,0)}$ is given by the expression (2), and the effective optical phonon mediated interaction is approximated by the Bardeen – Pines form [24, 25]. For the acoustic-phonon contribution to the effective potential, we also apply the Bardeen-Pines approximation, as in Ref. [26]:

$$V^{ac}(q, i\Omega) = -\frac{1}{\hbar} \left| V_{\mathbf{q}}^{(ac)} \right|^2 \frac{2\omega_{\mathbf{q}}}{\omega_{\mathbf{q}}^2 + \Omega^2}. \quad (24)$$

There are indications from experiment [2, 3, 5, 6] that the superconducting phase transition in a $\text{LaAlO}_3\text{-SrTiO}_3$ heterostructure is governed by the Berezinskii – Kosterlitz – Thouless (BKT) mechanism [27–29]. It is shown in Refs. [3, 6] that the temperature dependence of the resistance just above T_c is specific for a BKT phase transition, corresponding to the 2D nature of the superconducting system.

The critical temperature of the BKT phase transition is determined by the equation [28] which includes the pair superfluid density $\rho_s(T)$:

$$T_{BKT} = \frac{\pi}{4} \frac{\hbar^2}{k_B m_b} \rho_s(T_{BKT}). \quad (25)$$

The superfluid density monotonously decreases with increasing temperature, and turns to zero at $T = T_c$. Therefore, the critical temperature T_{BKT} must be necessarily lower than T_c . In the case when the BKT transition is present in the $\text{LaAlO}_3\text{-SrTiO}_3$ heterostructure, T_c can be interpreted as the pairing temperature at which the preformed pairs appear. In the $\text{LaAlO}_3\text{-SrTiO}_3$ heterostructures, the superfluid density n_s extracted from the BKT equation (25) is several orders of magnitude lower than the actual electron density: $n_s \ll n_0$. This inequality can be satisfied only when the gap parameter Δ is very small compared to its value at $T = 0$, and, consequently, when $(1 - T_{BKT}/T_c) \ll 1$. Therefore, as already concluded in Ref. [2], T_c and T_{BKT} are extremely close to each other in the $\text{LaAlO}_3\text{-SrTiO}_3$ heterostructures.

III. RESULTS AND DISCUSSION

For the numerical calculations, we use the set of material parameters already used in earlier works [17, 26]. The dielectric constants for SrTiO_3 are $\epsilon_{1,\infty} = 5.44$ and $\epsilon_{1,0} = 186$ (calculated using the Lyddane-Sachs-Teller relation for the LO- and TO- phonon frequencies and the ratio $\epsilon_0/\epsilon_\infty$). The effective mass for the present calculation has been taken $m_b = 1.65m_0$ [17] (where m_0 is the electron mass in vacuum). The dielectric constants for LaAlO_3 are used from Ref. [30]: $\epsilon_{2,\infty} = 4.2$ and $\epsilon_{2,0} = 24$. The only material parameter which is not yet well-determined, is the acoustic deformation potential D in strontium titanate. It should be noted that the deformation potential responsible for the interaction of an electron with the acoustic phonons is the “absolute” rather than “relative” deformation potential [31–33]. In the literature, we can find several different suggestions on the values of the deformation potential in strontium titanate. Koonce *et al.* [34] applied the value $D \approx 15$ eV to fit the experimental data on T_c in bulk strontium titanate. In Ref. [35] the deformation potential is estimated to be $D \approx 2.9$ eV on the basis of the value of the Fermi energy of the electrons. In Ref. [36] the value $D \approx 4$ eV is calculated on the basis of first principles density functional theory, that seems to be more reliable than two other values, because the many-valley band model of

Ref. [34] is not confirmed by later studies, and the deformation potential of Ref. [35] is a rough estimation using the Fermi energy of the electrons. As we discuss below, the results from our theory compare favorably with D values of [35, 36], but are incompatible with the large D value used in [34].

Here we have calculated T_c in the $\text{LaAlO}_3\text{-SrTiO}_3$ heterostructure using several values of the deformation potential: $D = 3$ eV, $D = 4$ eV and $D = 5$ eV. They seem to be physically reasonable, because they lie in the same range as the values used in Refs. [35, 36]. For the comparison of the calculated critical temperatures with the known experimental data, we use in the numeric calculations the model of the $\text{LaAlO}_3\text{-SrTiO}_3$ heterostructure accounting for the presence of an electrode at the oxide layer.

In Fig. 1, the kernel function $K(\omega, \omega')$ is plotted for the set of parameters indicated above, choosing the deformation potential $D = 4$ eV suggested in Ref. [36]. This kernel function is qualitatively similar to the kernel function for a 2D electron gas from Ref. [14]. There exists a distinction between the kernel functions for the 2D and 3D systems within the Kirzhnits – Takada method: for a 3D electron gas, the kernel function $K(0, \omega)$ tends to zero when $\omega \rightarrow -\epsilon_F$ achieving a local maximum in the interval $-\epsilon_F < \omega < 0$. On the contrary, for a 2D electron gas, $K(\omega, \omega')$ is a monotonically decreasing function of ω and ω' in the range of negative frequencies.

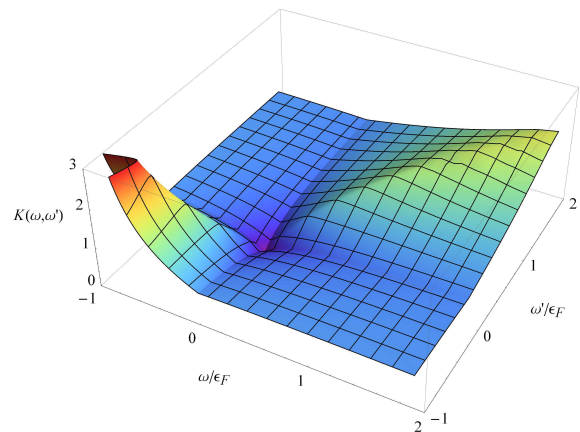


FIG. 1: Kernel function $K(\omega, \omega')$ for the $\text{LaAlO}_3\text{-SrTiO}_3$ structure using the set of parameters described in the text.

As explained in Refs. [13–15], superconductivity in an electron-phonon system can exist despite the fact that the kernel function $K(\omega, \omega')$ is positive for all frequencies. The kernel for energies larger than ϵ_F is dominated by the Coulomb repulsion between two electrons whose spatial distance is small, while the behavior of the kernel near the Fermi surface is due to both the Coulomb interaction and the attraction mediated by the plasmon-phonon excitations, between two electrons whose distance is rather large. Consequently, when, for example, $K(\epsilon_F, 0)$ is much larger than $K(0, 0)$, the two electrons

can avoid the region of the Coulomb repulsion and form a Cooper pair. We can see that, although $K(0,0)$ is not exactly equal to zero, $K(\omega, \omega')$ achieves its minimum at $\omega, \omega' = 0$, facilitating pairing.

The measured critical temperatures are taken from several sources [2–4]. The experimental work by N. Reyren *et al.* [2] contains only two points: $T_c \approx 0.1$ K for a 2D density of the electrons $n \approx 1.5 \times 10^{13} \text{ cm}^{-2}$, and $T_c \approx 0.2$ K for $n \approx 4 \times 10^{13} \text{ cm}^{-2}$. The paper [3] represents the critical temperature as a function of the gate voltage, and the dependence of the modulation of the electron density $\delta n(V)$ on the gate voltage. The total electron density is related to the modulation $\delta n(V)$ as $n(V) = n_0 + \delta n(V)$, where $n_0 \approx 4.5 \times 10^{13} \text{ cm}^{-2}$, according to Ref. [3]. Using the experimental data for $T_c(V)$ and $n(V)$ represented in these figures, we obtain the dependence $T_c(n)$ for the experiment [3]. We also include recent experimental results on the superconductivity in the $\text{LaAlO}_3\text{-SrTiO}_3$ heterostructure [4].

In Fig. 2 (a), the critical temperatures as a function of the 2D carrier density calculated in the present work are compared to the experimental data for $T_c(n)$ discussed above. It is worth noting that there exists a substantial difference between experimental values of T_c obtained in different experiments. However, they all are of the same order of magnitude and lie in the same range of the carrier densities.

The observed differences of the experimental results on the critical temperatures in the $\text{LaAlO}_3\text{-SrTiO}_3$ heterostructures can be explained as follows. In different experiments [2–4], the $\text{LaAlO}_3\text{-SrTiO}_3$ heterostructures have been grown independently. Therefore those heterostructures can at least slightly differ from each other. The thermal energy $k_B T_c$ is extremely small compared to the characteristic energies involved in the superconducting phase transition: the Fermi energy of the electrons and the LO-phonon energies (which both are of order ~ 100 meV). Under these conditions, the critical temperatures can be very sensitive to relatively small difference of the internal properties of the fabricated heterostructures. Additional factors (e. g., disorder, local phonons, defects, etc.) can substantially influence T_c . Moreover, also even the critical temperatures for bulk strontium titanate measured in different experiments [34, 37] differ substantially from each other. Consequently, the relatively large variation of the experimental results on the critical temperature in $\text{LaAlO}_3\text{-SrTiO}_3$ heterostructure is not surprising. Despite that uncertainty, the measured critical temperatures in different experiments are of the same order.

We can see that for each D , the curve is close to only few data points. However (i) experimental data are obtained with a substantial numeric inaccuracy, (ii) experimental data from different sources do not agree even with each other. It should be noted also that, since the thermal energy corresponding to the critical temperature in the LAO-STO structure is very small with respect to other energies participating in the superconductivity (the

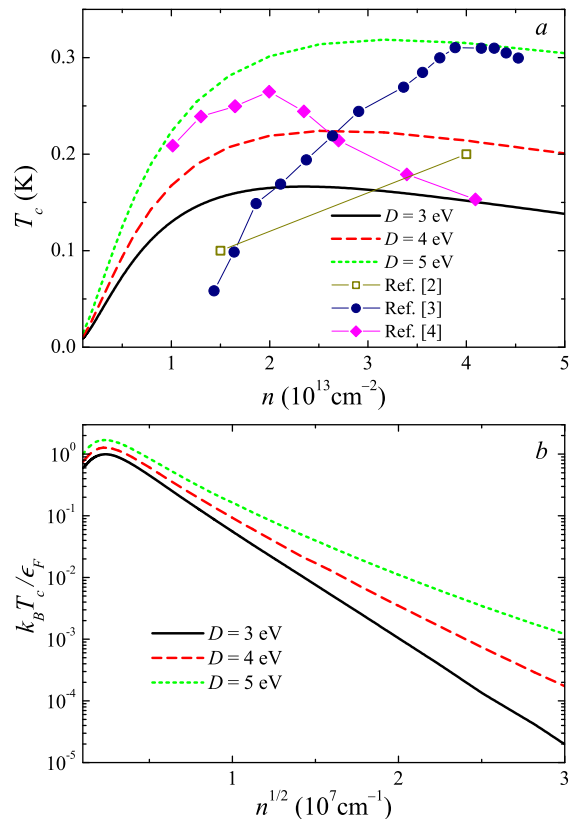


FIG. 2: (a) Critical temperature for the $\text{LaAlO}_3\text{-SrTiO}_3$ heterostructure as a function of the 2D electron density, compared to the experimental data extracted from Refs. [2–4]. (b) The calculated critical temperatures divided by the Fermi energy ϵ_F , plotted as a function of $n^{1/2}$.

optical-phonon energies and the Fermi energy), even a small uncertainty of these parameters can then lead to a significant change of the critical temperature. Our calculation, performed without fit using parameter values known from literature, yields the critical temperatures within the same range as in the experiments. We can therefore conclude that, taking into account the uncertainty of the experimental results on the critical temperatures, the suggested theoretical explanation of the superconducting phase transition in the $\text{LaAlO}_3\text{-SrTiO}_3$ heterostructures leads to tentative agreement with experiment.

We can see different regimes of T_c as a function of density in Fig. 2. First, the critical temperature exhibits almost linear dependence at small n up to $n \sim 10^{13} \text{ cm}^{-2}$. After reaching the maximum, as seen from Fig. 2 (b), the critical temperature falls down at high densities as $\sim n \exp(-c\sqrt{n})$ with a positive constant c depending on the parameters of the system. This density dependence of T_c for low and high densities can be explained as follows.

In the limit of low densities, the effective interaction potential $V^R(q, i\Omega)$ given by (22) tends to the non-screened effective interaction potential $V_0^R(q, i\Omega)$ that

does not depend on the density. Also the contribution $V^{ac}(q, i\Omega)$ to the total effective interaction due to the acoustic phonons is density-independent. Therefore at low densities the parameters λ tends to a constant depending on the material parameters of the system. According to (19), the critical temperature in the low-density limit is proportional to the carrier density.

This result has a clear physical interpretation. Let us compare (19) with the known BCS expression [39],

$$T_c \approx 1.14 \hbar \omega_D \exp \left(-\frac{1}{N(\epsilon_F) V} \right), \quad (26)$$

where ω_D is the Debye frequency, $N(\epsilon_F)$ is the density of states at the Fermi energy, and V is the model BCS matrix element. The BCS theory describes the adiabatic regime when $\hbar \omega_D \ll \epsilon_F$, and pairing occurs for the electrons whose energies lie in the layer of width $\delta \epsilon \sim \hbar \omega_D$ near the Fermi energy. As a result, $T_c \propto \hbar \omega_D$ within the BCS picture. On the contrary, in strontium titanate and in the $\text{LaAlO}_3\text{-SrTiO}_3$ heterostructure at low densities the anti-adiabatic regime is realized: $\epsilon_F \ll \hbar \omega_{L,j}$, where $\omega_{L,j}$ is an optical-phonon frequency. In the anti-adiabatic regime, all electrons participate in the superconductivity. Therefore the factor $\hbar \omega_D$ in the adiabatic regime corresponds to the factor ϵ_F in the anti-adiabatic regime.

Because in the anti-adiabatic regime all electrons contribute to superconductivity, the parameter λ hardly can be interpreted as $N(\epsilon_F) V$. In a non-adiabatic regime λ must be, in general, a functional of the density of states for all energies $0 < \epsilon < \epsilon_F$. However, the density of states for a 2D system and for a sufficiently low energy (where the band nonparabolicity is relatively small) is

$$N(\epsilon) = \frac{m_b}{\pi \hbar^2}, \quad (27)$$

so that $N(\epsilon)$ (and hence also λ) does not depend on the carrier concentration at low concentrations. Thus the aforesaid qualitative physical estimation leads to the low-density behavior $T_c(n) \propto n$, in agreement with the result obtained in the present work.

In the opposite regime of high carrier densities, the plasma frequency can exceed both the Fermi energy and the optical phonon energies. In this regime, the plasmon mechanism of superconductivity [14] must dominate. According to Ref. [14], the critical temperature for an electron gas in 2D with the effective mass m_b and the dielectric constant ϵ due to the plasmon mechanism can be modeled by an analytic expression,

$$T_c = \frac{2}{\pi} e^\gamma \epsilon_F \exp \left[-\frac{(1 + \langle F \rangle)^2}{\langle F^2 \rangle - K(0, 0)} \right] \quad (28)$$

with the averages

$$\langle A \rangle \equiv \int_{-\epsilon_F}^{\epsilon_F} \frac{d\omega}{2|\omega|} A(\omega) \quad (29)$$

and the function

$$F(\omega) = \frac{1}{4\pi g_v} \sqrt{\frac{q_{TF}}{p_F}} B\left(\frac{1}{4}, \frac{1}{2}\right) \sqrt{\frac{|\omega|}{\epsilon_F}}. \quad (30)$$

Here, $B(x, y)$ is the Euler beta function, g_v is the conduction band degeneracy, p_F is the Fermi momentum, and q_{TF} is the Thomas-Fermi wave vector. For a 2D electron gas, $q_{TF} = 2g_v e^2 m_b / \epsilon$ does not depend on the carrier density. Here, the factor g_v is equal to 1 because the conduction band in SrTiO_3 is split due to the spin-orbit interaction [40].

After the integration in (29), the critical temperature (28) takes the form

$$T_c = \frac{2}{\pi} e^\gamma \epsilon_F \exp \left[-\frac{(1 + 2C)^2}{C^2 - K(0, 0)} \right], \quad (31)$$

where C is given by:

$$C = \frac{1}{2\pi} B\left(\frac{1}{4}, \frac{1}{2}\right) \sqrt{\frac{q_{TF}}{p_F}}. \quad (32)$$

The upper bound for the density when $T_c = 0$ is determined by the equation

$$C^2 - K(0, 0) = 0. \quad (33)$$

The parameter C is proportional to $n^{-1/4}$, and $C \ll 1$ for sufficiently high densities. Therefore in the high-density range, but for densities smaller than that determined by (33), the model critical temperature (28) due to the plasmon mechanism behaves approximately as

$$T_c \approx \frac{2}{\pi} e^\gamma \epsilon_F \exp \left(-1.43554 \frac{p_F}{q_{TF}} \right). \quad (34)$$

Since $p_F = \sqrt{2\pi n}$, the estimation (34) following Ref. [14] is in agreement with the critical temperature obtained in the present work, as seen from Fig. 2 (b). In the figure, the ratio $k_B T_c / \epsilon_F$ is plotted in the logarithmic scale as a function of $n^{1/2}$, focusing at the high-density range (larger than in the experiments [2–4]). We can see that at relatively small acoustic deformation potential $D = 3$ eV, the dependence $\ln T_c$ as a function of $n^{1/2}$ is almost linear for high densities. For larger D , the acoustic-phonon mechanism stronger influences the density dependence of T_c leading to deviations from the purely plasmon picture.

IV. CONCLUSIONS

In conclusion, we have re-formulated the Kirzhnits method for a multilayer structure with several polar layers. The developed technique is capable to describe superconductivity in multilayer structures, where the electrostatic electron-electron interaction, the optical-phonon spectra, and the amplitudes of the electron-phonon interaction are modified compared to bulk. In

the present treatment, all phonon branches existing in the multilayer structure are taken into account.

We have found that at low densities, the critical temperature is well described by a BCS-like expression with the Fermi energy instead of the Debye energy. This is a direct consequence of the anti-adiabatic regime, which occurs at low carrier densities. At high densities, the density dependence of the critical temperature shows the domination of the plasmon mechanism of superconductivity.

The obtained agreement of the calculated critical temperatures with experiment gives support to the hypothesis that the mechanism of superconductivity is provided by the electron – optical-phonon interaction (see, e. g., [38]), at least in the multilayer structure analyzed in the present work.

Acknowledgments

We thank H. Boschker for the experimental data on critical temperatures and for discussions. We are grateful to M. Cohen, A. Zunger and C. G. Van de Walle for data on the deformation potential resulting from their works. This work was supported by FWO-V projects G.0370.09N, G.0180.09N, G.0119.12N, G.0122.12N, the WOG WO.035.04N (Belgium), the SNSF through Grant No. 200020-140761 and the National Center of Competence in Research (NCCR) “Materials with Novel Electronic Properties-MaNEP”.

-
- [1] A. Ohtomo and H.Y. Hwang, *Nature (London)* **427**, 423 (2004).
 - [2] N. Reyren, S. Thiel, A. Caviglia, L. Fitting Kourkoutis, G. Hammerl, C. Richter, C. Schneider, T. Kopp, A.-S. Rüetschi, D. Jaccard, M. Gabay, D. Muller, J.-M. Triscone, and J. Mannhart, *Science* **317**, 1196 (2007).
 - [3] A. Caviglia, S. Gariglio, N. Reyren, D. Jaccard, T. Schneider, M. Gabay, S. Thiel, G. Hammerl, J. Mannhart, and J.-M. Triscone, *Nature (London)* **456**, 624 (2008).
 - [4] C. Richter, H. Boschker, W. Dietsche, E. Fillis-Tsirakis, R. Jany, F. Loder, L. F. Kourkoutis, D. A. Muller, J. R. Kirtley, C. W. Schneider, and J. Mannhart, *Nature* **502**, 528 (2013).
 - [5] N. Reyren, S. Gariglio, A. D. Caviglia, D. Jaccard, T. Schneider, and J.-M. Triscone, *Appl. Phys. Lett.* **94**, 112506 (2009).
 - [6] T. Schneider, A. D. Caviglia, S. Gariglio, N. Reyren, and J.-M. Triscone, *Phys. Rev. B* **79**, 184502 (2009).
 - [7] G. M. Eliashberg, *Zh. Eksperim. i Teor. Fiz.* **38**, 966 (1960) [English transl.: *Soviet Phys.—JETP* **11**, 696 (1960)].
 - [8] D. J. Scalapino, J. R. Schrieffer, and J. W. Wilkins, *Phys. Rev.* **148**, 263 (1966).
 - [9] C. Grimaldi, L. Pietronero and S. Strässler, *Phys. Rev. Lett.* **75**, 1158 (1995).
 - [10] L. Pietronero, S. Strässler, and C. Grimaldi, *Phys. Rev. B* **52**, 10516 (1995).
 - [11] C. Grimaldi, L. Pietronero, and S. Strässler, *Phys. Rev. B* **52**, 10530 (1995).
 - [12] D. A. Kirzhnits, E. G. Maksimov and D. I. Khomskii, *J. Low Temp. Phys.* **10**, 79 (1973).
 - [13] Y. Takada, *J. Phys. Soc. Jpn.* **49**, 1267 (1980).
 - [14] Y. Takada, *J. Phys. Soc. Jpn.* **45**, 786 (1978).
 - [15] Y. Takada, *J. Phys. Soc. Jpn.* **49**, 1713 (1980).
 - [16] J. L. M. van Mechelen, D. van der Marel, C. Grimaldi, A. B. Kuzmenko, N. P. Armitage, N. Reyren, H. Hagemann, and I. I. Mazin, *Phys. Rev. Lett.* **100**, 226403 (2008).
 - [17] J. T. Devreese, S. N. Klimin, J. L. M. van Mechelen, and D. van der Marel, *Phys. Rev. B* **81**, 125119 (2010).
 - [18] D. N. Zubarev, *Sov. Phys. Uspekhi* **3**, 320 (1960); [Russian original: *Usp. Fiz. Nauk* **71**, 71 (1960)].
 - [19] N. Mori and T. Ando, *Phys. Rev. B* **40**, 6175 (1989).
 - [20] G. Q. Hai, F. M. Peeters and J. T. Devreese, *Phys. Rev. B* **42**, 11063 (1990).
 - [21] F. M. Peeters and J. T. Devreese, *Phys. Rev. B* **32**, 3515 (1985).
 - [22] D. Pines and P. Nozières, *Theory Of Quantum Liquids: Normal Fermi Liquids* (Addison-Wesley Publishing Company, Advanced Book Program, 1994).
 - [23] T. Ando, A. B. Fowler, and F. Stern, *Rev. Mod. Phys.* **54**, 437 (1982).
 - [24] J. Bardeen and D. Pines, *Phys. Rev.* **99**, 1140 (1955).
 - [25] M. J. Kelly and W. Hanke, *Phys. Rev. B* **23**, 112 (1981).
 - [26] S. N. Klimin, J. Tempere, D. van der Marel, and J. T. Devreese, *Phys. Rev. B* **86**, 045113 (2012).
 - [27] V. L. Berezinskii, *Sov. Phys. JETP* **32**, 493 (1971).
 - [28] J. M. Kosterlitz and D. J. Thouless, *J. Phys. C* **6**, 1181 (1973).
 - [29] J. M. Kosterlitz, *J. Phys. C* **7**, 1046 (1974).
 - [30] P. Calvani, M. Capizzi, F. Donato, P. Dore, S. Lupi, P. Maselli, and C. P. Varsamis, *Physica C* **181**, 289 (1991).
 - [31] M. Cardona and N. E. Christensen, *Phys. Rev. B* **35**, 6182 (1987).
 - [32] C. G. Van de Walle and R. M. Martin, *Phys. Rev. Lett.* **62**, 2028 (1989).
 - [33] A. Franceschetti, S.-H. Wei, and A. Zunger, *Phys. Rev. B* **50**, 17797 (1994).
 - [34] C. S. Koonce, M. L. Cohen, J. F. Schooley, W. R. Hosler, and E. R. Pfeiffer, *Phys. Rev.* **163**, 380 (1967).
 - [35] A. N. Morozovska, E. A. Eliseev, G. S. Svechnikov, and S. V. Kalinin, *Phys. Rev. B* **84**, 045402 (2011).
 - [36] A. Janotti, B. Jalan, S. Stemmer, and C. G. Van de Walle, *Appl. Phys. Letters* **100**, 262104 (2012).
 - [37] G. Binnig, A. Baratoff, H. E. Hoenig, and J. G. Bednorz, *Phys. Rev. Lett.* **45**, 1352 (1980).
 - [38] O. V. Dolgov, D. A. Kirzhnits, and E. G. Maksimov, *Rev. Mod. Phys.* **53**, 81 (1981).
 - [39] J. Bardeen, L. N. Cooper, and R. Schrieffer, *Phys. Rev.* **108**, 1175 (1957).
 - [40] D. van der Marel, J. L. M. van Mechelen, and I. I. Mazin, *Phys. Rev. B* **84**, 205111 (2011).